Physics of the Solid State, 2025, Vol. 67, No. 8

08,10

Formation of potassium clusters in electric field on the surface of a tungsten single crystal

© D.P. Bernatsky, V.G. Pavlov

Ioffe Institute,
St. Petersburg, Russia

E-mail: bernatskii@ms.ioffe.ru

Received May 26, 2025
Revised August 1, 2025
Accepted August 6, 2025

Formation of monatomic (K^+) and cluster potassium ions (K_2^+, K_3^+, K_4^+, K_5^+, K_6^+) in the process of field desorption from the spherical surface of a tungsten single crystal was detected. The studies were carried out in a field emission microscope, which provides for measuring the mass of ions desorbed by an electric field using time-of-flight mass analysis. The electric field strength required for potassium ions desorption corresponded to the calculated values obtained in the image force model for field desorption of alkali metals. For all detected potassium cluster ions, there is a minimum in the dependence of the number of desorbed ions on the electric field strength. For monatomic ions, such a minimum is not observed. The discovered patterns are explained by a shift in cluster desorption zones from the center of the sample to the periphery with increasing voltage.

Keywords: adsorption, field desorption, microscopy, ions, mass spectrometry.

DOI: 10.61011/PSS.2025.08.62273.142-25

1. Introduction

Interaction of various atoms adsorbed on a surface of the solid body is of interest for many fields of science and engineering, in particular, such as heterogeneous catalysis, crystal growth, nanotechnology, microelectronics. Formation of two-dimensional and three-dimensional associates (islands, clusters) on the surface is observed for the most adsorbates. The clusters of atoms and molecules of various substances are widely applied in various nanotechnologies [1,2]. In particular, the study [1] collects and discusses the latest innovations in the field of nanotechnologies for application in power engineering. It is noted that variation of a nanocluster size opens up interesting opportunities for designing materials with a certain functionality. The study [2] considers application of metal nanoclusters in technologies of storage and conversion of energy (solar cells, supercapacitors and batteries). Additionally, a lot of attention is paid in this study to application of mass-spectrometry methods of studies for determining a mass and a mechanism of growth of the metal nanoclusters.

Formation of the clusters of alkali metals on the surface of the metal is considered to be unlikely due to dipole-dipole interaction between atoms of the alkali metals adsorbed on the metal surface. It is especially pronounced in the region of submonolayer coatings, when an ionization potential of the adsorbed atom is less than a surface work function [3,4]. Quantum-mechanical and quasi-classical adsorption theories [4–7] have confirmed a dominant role of Coulomb dipole-dipole repulsion in interaction of the alkali metal atoms adsorbed on the metal surface in vacuum at small coatings.

The study [8] has discovered formation of cluster cesium ions (Cs_2^+, Cs_3^+, Cs_4^+, Cs_5^+) during field desorption from a nanostructured quasi-spherical surface of a rhenium single crystal in the region of the submonolayer coatings under high-vacuum conditions. The masses of the desorbed ions were determined using mass-spectrometry analysis that is based on measuring a time of flight of the ions from a specimen to a recording system. We also studied a dependence of a number of the formed atoms on the electric field strength. In this regard, it is interesting to study formation of clusters of other alkali metals on other substrates.

The present study investigates formation of potassium ion clusters in the electric field on a tungsten-single-crystal spherical surface that is heterogeneous in terms of the structure and the work function. The studies were carried out by means of field emission and desorption microscopy and time-of-flight mass-spectrometry analysis of the ions desorbed by the electric field [9–11]. It is known that formation of alkali metal ions during field desorption requires relatively low desorbing fields ($\sim 10^7$ V/cm) [12]. It is explained in an image force model for field desorption by the low ionization potential of the alkali metal atoms and a weak bond of the adsorbed atoms with the metal surface [11].

Cluster recording and investigation of their composition, properties and formation laws were carried out by means of field desorption. According to the image force model for field desorption, the cluster ions can form since the alkali metal clusters have lower ionization potentials as compared to the atoms [13].

2. Experimental methodology

The studies were carried out using a field electron and a field desorption microscope with time-of-flight mass analysis

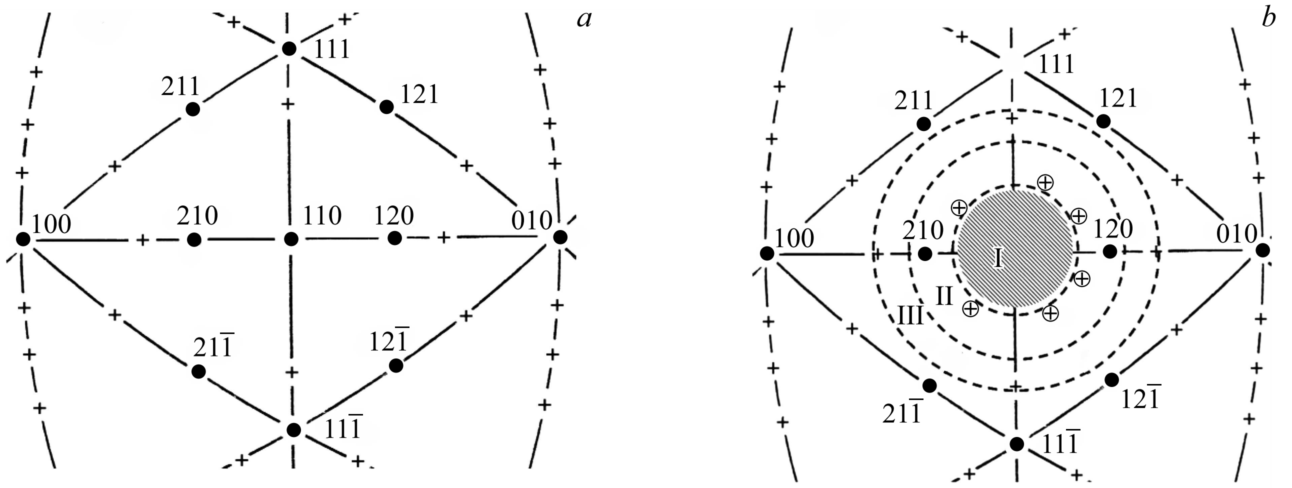

Figure 1. Standard projection for cubic crystals with the central axis (110) (a central part).

of the ions desorbed by the electric field [9]. The tungsten specimen is manufactured as a spike with the rounding radius of about $r_s \approx 500$ nm. A near-semi-sphere spike tip is a single crystal. A surface of the single crystal consists of crystalline planes of the size $1-100$ nm and steps of a monoatomic height.

An enlarged image of the spherical surface of the tungsten specimen is formed in a luminescent screen by field emission of electrons (the field electron microscope mode) or field desorption of adsorbate ions (the field desorption microscope mode) from the surface of the specimen. To register weak (electron or ion) currents from the specimen, an assembly of two microchannel plates (MP) of the diameter of 56 mm was placed in front of the luminescent screen. A distance from an entrance microchannel plate to the specimen surface was $r = 18$ cm. Then, a magnification ratio will be approximately equal to the ratio $r/r_s \approx 3.5 \cdot 10^5$ [14].

The specimen is manufactured from tungsten wire of the diameter of 0.1 mm, its one end is welded to a tungsten loop. Another end of the tungsten wire is loaded into a solution for electrochemical etching. Electrochemical etching resulted in formation of the spike. Then, in high vacuum (the pressure was $P \approx 5 \cdot 10^{-9}$ Torr), the specimen was annealed directly in the chamber of the field emission microscope at the temperature of $T = 2500$ K.

During annealing the specimen was cleaned, and a single-crystal quasi-spherical spike tip with the rounding radius of about 500 nm with flat low-index facets of the tungsten crystal was formed on the surface. Figure 1 shows a diagram of the planes in the standard projection for the cubic-lattice crystals with the central axis (110) [15,16] and designation of some low-index facets within a recording zone of the field electron microscope.

The formation of the single-crystal tip of an emitter was accompanied by appearance of a field electron image of tungsten, which is standard for the cubic-lattice crystals [14].

The measurement of the time of flight (t) of the desorbed ions from the surface of the specimen to a detector that consisted of the two multichannel plates and the luminescent screen made it possible to evaluate the mass of the desorbed ions. For this we used the formula

$$t = r_0\big(2q\Sigma U/m\big)^{-1/2}, \tag{1}$$

where r_0 — the distance from the specimen surface to the detector, q — the charge of the ion, $\Sigma U = U_0 + U_\mathrm{p}$ — the difference of potentials between the specimen and the microchannel plate, U_0 — the value of constant voltage applied to the specimen, U_p — the amplitude of pulsed voltage, m — the mass of a recorded ion [17]. Since the radius of the hemispherical surface of the specimen (as a spike) r_s (~ 500 nm) is significantly less than the distance to the microchannel plate, it can be assumed that all the energy $q\Sigma U$ is gained by the desorbed ion practically at the surface of the specimen.

The experimental setup is shown in Figure 2.

The difference of potentials ΣU between the specimen and the detector was created using adjustable constant voltage ($0-30$ kV) from the source *2* and pulsed voltage from the source *3* via decoupling capacitance C. Parameters of a voltage pulse could vary by the amplitude ($0-4$ kV) and duration ($10-20$ ns). By means of variation of voltage at the microchannel plate ($0.6-2.5$ kV), it was possible to adjust the amplification coefficient in various modes up to recording of single ions.

For field desorption of an adsorbed atom in the form of the singly-charged ion it is necessary to overcome the energy barrier $Q(F)$, which in the image force model is determined by the expression [18]:

$$Q(F) = \Lambda(\vartheta) + I - \varphi(\theta) - e^{3/2}F^{1/2} + \Delta E_\mathrm{p}(\theta), \tag{2}$$

where Λ — the heat of desorption of the atom, I — the ionization potential of the atom, φ — the surface work

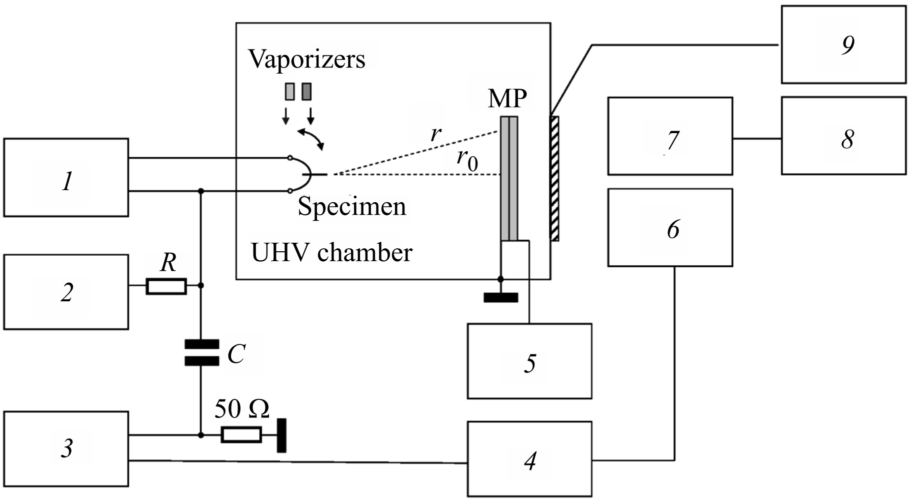

Figure 2. Experimental setup. *1* — the specimen heating unit, *2* — the adjustable high-voltage DC source, *3* — the adjustable generator of HV nanosecond pulses, *4* — the storage oscilloscope, *5* — the adjustable power supply unit of the microchannel plates, *6* — the photoamplifier, *7* — the video camera, *8* — the computer, *9* — the adjustable power supply unit of the luminescent screen.

function, e — the charge of the electron, F — the strength of the applied electric field, θ — the degree of coverage of by surface by the adsorbate, ΔE_p — the polarization correction that is equal to $1/2(\alpha_\mathrm{a} - \alpha_\mathrm{i})F^2$, where α_a — polarizability of the adsorbed atom, α_i — polarizability of the desorbed ion. For the adsorbed potassium atoms, polarizability α_a is small and does not exceed $5\,\mathrm{Å}^3$ [19], while for the desorbed potassium ion α_i does not exceed $1.2\,\mathrm{Å}^3$ [20]. The time τ requried for field desorption during thermal activation is determined by the Arrhenius equation

$$\tau = 1/\nu_o \exp(Q/k_\mathrm{B}T), \qquad (3)$$

where ν_0 — the vibration frequency, k_B — the Boltzmann constant, T — the temperature. It is possible to write an expression from the relationships (2) and (3) to estimate the value of the electric field strength F required for desorption of a selected adsorbate:

$$e^{3/2}F^{1/2} = \Lambda + I - \varphi - k_\mathrm{B}T\ln(\tau\nu_0). \qquad (4)$$

The value of the temperature correction $k_\mathrm{B}T\ln(\tau\nu_0)$ at the room temperature $T = 300\,\mathrm{K}$ is estimated to be within the $0.5{-}0.78\,\mathrm{eV}$ when assuming that $\nu_0 \approx 10^8{-}10^{13}\mathrm{s}^{-1}$ [18].

At the room temperature of the specimen, due to surface diffusion of the adsorbed potassium atoms, migration equilibrium of the potassium atoms is set on the surface that is heterogeneous in terms of the structure and the work function. The condition of migration equilibrium on the surface means that concentration of the adsorbate on various portions of the specimen surface can be different and it will depend on heat of evaporation of an adatom Λ. The more Λ, the higher surface concentration of the adsorbate on a given portion of the surface [21]. The mode of migration equilibrium of the adsorbate on the specimen surface is characterized in that during desorption of the adatoms from the surface the adsorbate concentration is restored on the specimen tip due to diffusion of the adatoms into the desorption zone in the heterogeneous electric field. As the specimen is a cone with the quasi-spherical tip, the electric field on its surface is heterogeneous and the largest strength is within the facet (110) (Figure 1).

As a result of this, when achieving a threshold value desorption of the adsorbate starts from this region as an avalanche-like flash (the hatched region in Figure 1, *b*). This is attributable to the fact that with decrease of the concentration of the alkali metal atoms on the surface, as a result of field desorption the work function increases, the energy barrier $Q(F)$ decreases and a desorption rate that is determined by the expression (3) increases. As a result, the central region of the specimen is free of the adsorbate in an avalanche-like manner. Due to diffusion of the potassium adatoms in the inhomogeneous electric field to the tip (provided that there is migration equilibrium of the adsorbate), they are desorbed at a boundary of the central region (Figure 1, *b*), i. e. where the electric field strength has the threshold value (the zone I, Figure 1, *b*). At the same time, unless the voltage on the specimen is changed, field desorption can proceed for quite long time due to diffusion of the adatoms from a specimen periphery. With increase of voltage on the specimen the desorption zone will be shifted toward the periphery (the zone II, the zone III, Figure 1, *b*) and field desorption may go beyond recording limits.

In order to measure the masses of the potassium ions that are desorbed in the electric field, the specimen is energized with constant voltage (whose value is close to a desorption-threshold value) and a voltage pulse that stimulates desorption. The voltage pulse from the generator *3* (Figure 2) enters the specimen and simultaneously starts sweep of the storage oscilloscope *4*. In the time of flight t the desorbed potassium ions hit the detector and are amplified in the microchannel plate and the luminescent screen forms a light flash that is recorded by the photomultiplier tube *6*, where the voltage pulse is formed to be supplied to the storage oscilloscope. By measuring the time of flight of the ions t on calibrated sweep of the oscilloscope, we can evaluated the mass of the desorbed ions. Due to the fact that in the field desorption microscope the desorbed ions move along radial trajectories from the quasi-spherical surface of the sample and the detector is a flat surface of the microchannel plate, the distances from the specimen to the microchannel plate for the ions desorbed from various parts of the surface will be different (r_0 and r in Figure 2). It will introduce some uncertainty in identification of large polyatomic clusters ($N > 10$). If necessary, this uncertainty can be decreased by limiting a recording region using diaphragms.

3. Results and discussion

In order to determine the electric field strength F on the studied surface of the specimen, we have calculated a factor of the electric field β based on the experimentally obtained Fowler–Nordheim characteristics [15]. The value of β for the field emitter used in the experiments turned out to be $\beta = 5600\,\text{cm}^{-1}$. The electric field strength F was determined by the formula $F = \beta U$, where U is voltage on the specimen. The voltage on the specimen could be increased to 30 kV, which corresponded to the maximum value of F on the surface of the specimen $\sim 1.7 \cdot 10^8$ V/cm. In order to evaluate a degree of coverage θ of the specimen surface by potassium, we took the dependence of the work function φ on the time of potassium sputtering. This dependence that is typical for alkali and alkaline earth metals passes through the minimum in the region of optimal coverage. The work function of the specimen during sputtering of the alkali metal atoms can be determined by the formula

$$\varphi = \varphi_0 (U/U_0)^{2/3}, \tag{5}$$

where φ_0 — the work function of the surface of the pure tungsten specimen ($\varphi_0 = 4.5$ eV), U_0 — voltage on the pure specimen, U — voltage on the specimen during adsorption of the potassium atoms, which is measured at the same current of field electron emission from the emitter [22].

According to the expression (4), the value of the desorbing field has a minimum value at the high work function of the specimen surface, which corresponds to minimum values of surface coverage by potassium (the degree of coverage $\theta \approx 0.1$). For theoretical evaluation of the electric field strength required for desorption at a selected small potassium coating ($\theta \approx 0.1$), we assume that the work function of the tungsten specimen's surface is $\varphi = 4.5$ eV, $\Lambda = 2.7$ eV [22].

Figure 3 exemplifies the time-of-flight mass spectra that are obtained during field desorption of potassium from tungsten at the room temperature of the specimen. Each of the spectra can have at least one peak. The mass spectra were obtained within the range of voltages $\Sigma U = U_0 + U_\text{p}$ from 5 to 7 kV, which coincides with the values obtained by the formula (4).

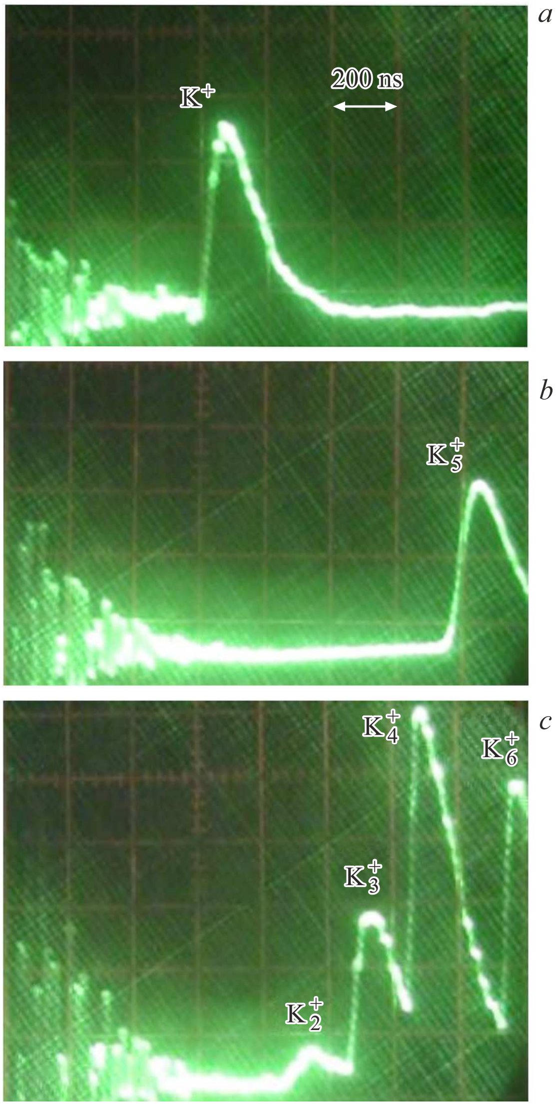

Figure 3. Mass spectra of the potassium ions. The spectra could contain *a*) monoatomic ions, *b*) single clusters or *c*) several clusters.

Processing of arrays of the spectra obtained at various voltages at the specimen for the monoatomic ions of cesium [2] and potassium is shown in Figure 4. The abscissa axis has a total voltage $\Sigma U = U_0 + U_\text{p}$ applied to the specimen, while the ordinate axis exhibits the frequency of appearance of the peaks of the monoatomic ions of potassium and cesium.

By substituting the values of φ, Λ, the temperature correction $\Delta E_\text{T} = 0.78{-}0.5$ eV and the ionization potential of the potassium atom $I = 4.34$ eV into the expression (4), we obtain an interval of the desorbing field strengths $F = 2.8{-}3.8 \cdot 10^7$ V/cm.

As it is clear in the provided graph, the dependences of field desorption of potassium on tungsten and of cesium on rhenium are of the same form. The threshold values of the

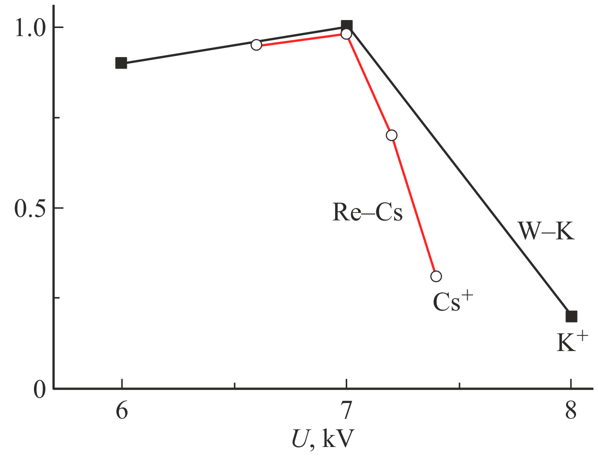

Figure 4. Frequency of appearance of the monoatomic ions of potassium and cesium in the spectra in a dependence on voltage on the specimen.

electric field strength for desorption are first achieved in the central region of the specimen (the region I, Figure 1, *b*). Avalanche-like desorption from this region occurs and it is preserved from the boundary of this region due to diffusion of the adatoms to the specimen (spike) tip in the heterogeneous electric field. With increase of voltage on the specimen, the desorption boundary is shifted towards the specimen periphery (the regions II and III, Figure 1, *b*). With a certain voltage on the specimen, there is drop of field desorption both for the monoatomic ions of potassium as well as for the monoatomic ions of cesium. It can be due to increase of a local activation barrier of field desorption $Q(F)$ on the surface and exit of desorption out of the recording region.

In the experimental conditions, potassium vapor pressures are much less than 10^{-9} Torr and it means that it is almost impossible for the atoms or clusters of potassium to leave vacuum and hit the desorption region on the surface for the time of the desorbing pulse of duration of 10 ns. Therefore, all the processes of formation of the cluster ions occur on the surface.

For the cluster ions of cesium [2] and potassium, the dependences of the frequency of appearance of the peaks in the mass spectra on voltage on the specimen are shown in Figure 5 (*a* — for potassium, *b* — for cesium). It is clear from the provided graphs that within the recording region of the desorbed ions from the specimen the frequency of appearance of a cluster ion depends not only on its mass, but on the desorption zone as well (localization on the surface) in a dependence on the applied voltage.

It is reasonable to assume that the monoatomic ions are formed only at the surface portions, in which the threshold value of the electric field for desorption is achieved. Under conditions of migration equilibrium, the potassium adatoms are located everywhere on the surface. Consequently, one should not expect a strong dependence of desorption of the monoatomic ions on applied voltage within the recording region.

For field desorption of the clusters, the threshold value of the electric field strength can be even less than for the monoatomic ions due to smaller cluster ionization potentials. In particular, it is reflected for potassium in reduction of desorbing voltages on the specimen (Figure 5, *a*) as compared to the monoatomic ions. But for potassium there is a clear dependence (a minimum on the graph) of the frequency of appearance of the polyatomic ions on voltage on the specimen within the recording zone. It is also manifested for cesium, but more weakly. Apparently, the found dependence reflect the fact that in addition to applied voltage, field desorption also requires a sufficient concentration of the polyatomic clusters on the surface. Since with increase of voltage the desorption zone is moved from the center towards the periphery, it is quite likely that the change of the frequency of appearance of the peaks of the cluster ions indicates the change of the their concentration on the surface.

The structures of the adsorbed alkali metal atoms on the metal surfaces are experimentally investigated in the review study [23]. The studies performed by the low-energy electron diffraction method have shown that dipole-dipole repulsion is the main in interatomic interaction for the

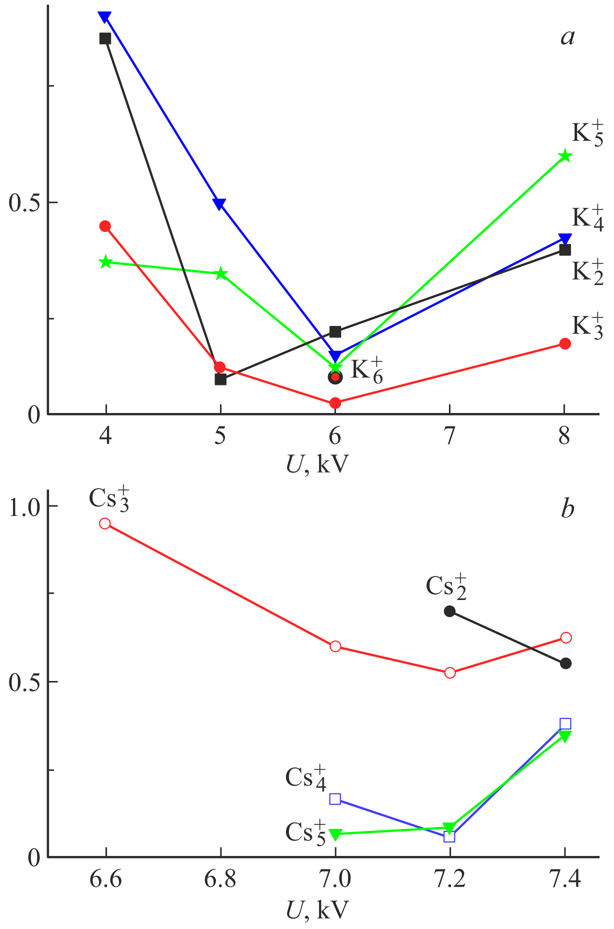

Figure 5. Frequency of appearance of the peaks of the cluster ions in the mass spectra in a dependence on voltage on the specimen: *a*) of potassium and *b*) of cesium.

submonolayer coatings. It was found for grooved facets in some systems that linear chains were formed perpendicular to a groove direction, thereby indicating indirect interatomic interaction. However, these structures were not observed for the potassium adatoms.

Probably, cluster formation on the complex surface is affected by presence of monoatomic steps as well as by presence of various crystalline planes and diffusion of the adatoms in the heterogeneous electric field.

4. Conclusion

1. The time-of-flight mass-spectrometry analysis and field desorption microscopy were used to show that the potassium clusters were formed on the quasi-spherical surface of the tungsten single crystal.

2. The monoatomic (K^+) and the polyatomic potassium ions (K_2^+, K_3^+, K_4^+, K_5^+, K_6^+) are recorded at the submonolayer coating and the electric field strength $\sim 10^7$ V/cm.

3. We have found a non-monotonic dependence of the number of the formed ion clusters of potassium on the electric field strength, thereby reflective different efficiency of cluster formation when changing the desorption zones on the surface.

4. The ion clusters of potassium are formed with the smaller electric field strength as compared to the monoatomic ions, which can be related to decrease of the cluster ionization potential.

Funding

The study was carried out under state assignment on topic FFUG-1024-0030.

Conflict of interest

The authors declare that they have no conflict of interest.

References

[1] Nano Tools and Devices for Enhanced Renewable Energy / Eds S. Devasahayam, C.M. Hussain. Elsevier, Amsterdam (2021). 598 p.

[2] Luminescent Metal Nanoclasters. Synthesis, Characterization, and Applications / Eds S. Thomas, K. Joseph, S. Appukuttan, M.S. Mathew. Elsevier, Amsterdam (2022). 704 p.

[3] L.A. Bol'shov, A.P. Napartovich, A.G. Naumovets, A.G. Fedorus. Sov. Phys. Uspekhi **20**, *5*, 432 (1977).

[4] A.G. Naumovets. Physica A **357**, *2*, 189 (2005).

[5] S.G. Davison, K.W. Sulston. Green-Function Theory of Chemisorption. Springer, Berlin (2006). 211 p.

[6] S.Yu. Davydov, A.A. Lebedev, O.V. Posrednik. Elementarnoye vvedeniye v teoriyu nanosistem. Lan', SPb (2022). 192 s. (in Russian). ISBN 978-5-8114-1565-6

[7] S.Yu. Davydov, A.V. Zubov. Phys. Solid State **62**, *8*, 1469 (2020).

[8] D.P. Bernatskii, V.G. Pavlov. FTT **66**, *7*, 1208 (2024). (in Russian).

[9] D.P. Bernatskii, V.G. Pavlov. Bull. RAS. Phys. **73**, *5*, 673 (2009).

[10] Y. Suchorski. Field Ion and Field Desorption Microscopy: Principles and Applications. Springer-Verlag, Berlin (2015). 272 p.

[11] E.W. Müller, T.T. Tsong. Field Ion Microscopy, Field Ionization and Field Evaporation. Pergamon Press, Oxford, N.Y. (1973). 139 p.

[12] D.P. Bernatskii, V.G. Pavlov. Tech. Phys. Lett. **44**, *2*, 178 (2018).

[13] P.J. Foster, R.E. Leckenby, E.J. Robbins. J. Phys. B: Atom. Mol. Phys. **2**, *4*, 478 (1969).

[14] A.N. Dobretsov, M.V. Gomoyunova. Emissionnaya elektronika. Nauka, M., (1966). 559 p. (in Russian).

[15] Field Ion Microscopy / Eds J.J. Hren, S. Rangathan. Plenium Press, N.Y. (1968).

[16] E.W. Müller, T.T. Tsong. Field Ion Microscopy. Elsevier, N.Y. (1969).

[17] J.A. Panitz. Progress. Surf. Sci. **8**, *6*, 219 (1978).

[18] E.W. Müller. Adv. Electron Phys. **13**, 83 (1960).

[19] E.V. Klimenko, A.G. Naumovets. FTT **13**, *1*, 33 (1971). (in Russian).

[20] A. Dalgarno. Adv. Phys. **11**, *44*, 281 (1962).

[21] V.N. Shrednik, E.V. Snezhko. FTT **6**, *11*, 3409 (1964). (in Russian).

[22] R. Schmidt, J. Gomer. J. Chem. Phys. **42**, *10*, 3573 (1965).

[23] O.M. Braun, V.K. Medvedev. Sov. Phys. Uspekhi **32**, *4*, 328 (1989).

Translated by M.Shevelev